ACS APPLIED MATERIALS & INTERFACES

RESEARCH ARTICLE

www.acsami.org

Preparation SnO_2 Nanolayer on Flexible Polyimide Substrates via Direct Ion-Exchange and in situ Oxidation Process

Guanghui Cui,[†,‡] Dezhen Wu,[‡] Shengli Qi,[†] Shao Jin,[†] Zhanpeng Wu,[*,†,‡] and Riguang Jin[†]

[†]Key Laboratory of Carbon Fiber and Functional Polymers, Ministry of Education, Beijing University of Chemical Technology, Beijing 100029, China

[‡]State Key Laboratory of Chemical Resource Engineering, Beijing University of Chemical Technology, Beijing 100029, China

ABSTRACT: Tin oxide (SnO_2) nanolayers were formed on flexible polyimide (PI) substrate via direct ion-exchange and in situ oxidation process utilizing pyromellitic dianhydride/4, 4′-oxidianiline-based poly(amic acid) films as polyimide precursor. During an ion-exchange process, stannous ions were doped into the precursor by immersion in ethanolic solution of stannous chloride. Subsequent thermal treatment of the tin(II)-containing precursor at a constant heating rate not only imidized poly(amic acid) to PI but also converted stannous ions into SnO_2 clusters, which diffused and aggregated onto the surface of polymer matrix, forming continuous tin oxide layers. Inductively coupled plasma (ICP) was used to investigate the ion-exchange process. Changes in chemical structure of the poly(amic acid) film and the crystal structure of tin oxides were analyzed by attenuated total reflection-Fourier transform infrared (ATR-FTIR) and X-ray diffraction (XRD). Scanning electron microscopy (SEM) and transmission electron microscopy (TEM) were used to study the microstructure of the PI/SnO_2 nanocomposite films. The nanocomposite film maintained essential mechanical property and thermal stability of pristine PI films.

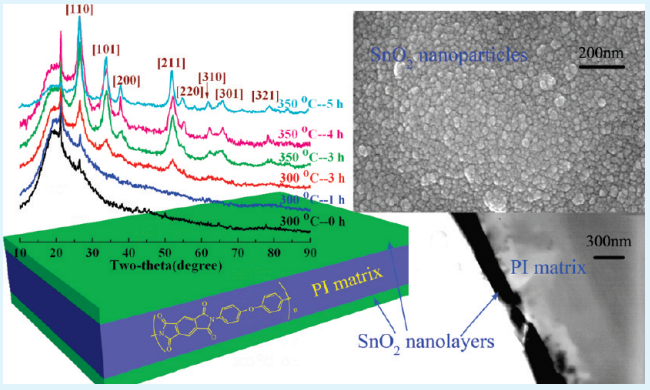

KEYWORDS: polyimide, tin oxide, direct ion exchange, in situ oxidation, nanocomposite film

INTRODUCTION

Fabrication of electronic components onto various material surfaces, particularly onto polymeric surfaces,[1−16] has been attracting increasing attention due to several distinctive properties of nanoparticles and anomalous cooperative properties of systems. Among polymeric materials, polyimide (PI) is a promising candidate for the matrix due to its attractive properties including excellent tensile strength and modulus, low thermal expansivity and dielectric constant, high thermal stability, and good resistance to organic solvents.[17,18] Fabrication of metal oxides nanoparticles onto flexible PI surfaces is still of great interest because of their various practical applications, such as in flexible flat panels and wearable displays, phosphors, piezoelectric, ferroelectric, organic electronic, solar cells, and ferromagnetic elements.[1,13−16,19−22]

General approaches of fabrication of polymer/metal-oxide composite films are ex situ methods,[2−4,13,14,23] which involves external precipitation of metal oxide nanoparticles by physical and/or chemical methods, and then followed by consolidation of the materials. The shortcomings of such approaches are that the formation of relatively coarse particles leads to large and inhomogeneous oxide powders. An alternative method for preparing uniformly distributed metal oxide nanaoparticles in polymeric substrates is to synthesize metal oxide materials in situ while preparing the polymeric substrates. A typical preparation involves dissolving of metal salts or complex in polymeric precursor solution and decomposition to corresponding metal oxides while thermal curing the films.[19,24−30] However, this method suffers from the drawback that metal complex would remained in the polymeric substrates during the whole procedures, which leads to a degradation of the polymeric matrix.[24,25] Thus, metal oxide precursors containing strong acids groups, such as Cl^-, SO_4^{2-} and NO_3^-, should be avoided, and the moderate organic acid groups with appropriate concentration should be used. In the 1990s, Taylor and co-workers reported that the prepared PI/Fe_2O_3 film, through dissolving of iron(III) acetylacetonate in poly(amic acid) (PAA) *N*,*N*-dimethylacetamide (DMAc) solution, was found very brittle after thermal treatment when the concentration of metal ions was more than 4 wt %.[24]

We previously reported that PI/nickel-oxide films were fabricated through surface modification and ion-exchange technique.[31] The method mainly relies on chemical surface modification of commercial PI films to form cation exchangeable sites (i.e., carboxylate) and subsequent incorporation of nickel ions via ion-exchange reactions. Subsequent deposition process in urea solution made nickel ions convert to $Ni(OH)_2$ which decomposed to the layer consisting of NiO nanoparticles and PI matrix during final thermal treatment in air. In this method, most

Received: November 22, 2010
Accepted: February 15, 2011
Published: March 03, 2011

Scheme 1. Ideal illustrative Procedures for Preparation of PI/SnO_2 Nanocomposite Films via Direct Ion-Exchange and in situ Oxidation Process[a]

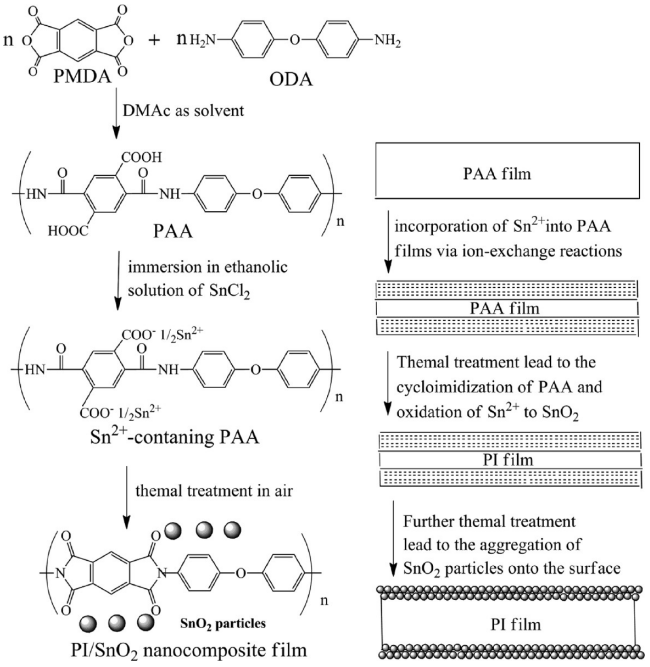

[a] The right flow diagrams are observed from a cross-sectional view.

common water-soluble nickel salts containing strong acid radicals, such as sulfate, carboxylate, and nitrate, can be used as NiO precursors. During ion exchange in aqueous nickel salt solution, only positive ions are exchanged into the polymeric matrix, with no risk of strong acid radical being incorporated into the films. However, it still has obstacles that we have to use the commercial PI films, which led to multistep fabricating processes and each step has to be precisely controlled to avoid peeling off metal oxide overlayers from PI substrates.

To overcome these problems, we recently reported that surface silver metallized PI films could be prepared through a direct ion-exchange self-metallization technique.[32−34] "Direct ion-exchange" refers to the development of silver(I)-containing PAA films, which are obtained by directly immersing damp-dry PAA films into an aqueous silver(I) solution to perform ion-exchange reactions. Subsequent thermal treatment of the silver-(I)-PAA films induces reduction of silver ions to give the metallized surfaces without additional reducing agent. We now report extension of our direct ion-exchange technique to metal oxide layers on flexible PI substrates. We selected tin oxide (SnO_2) as a model metal oxide, since it is an *n*-type functional semiconducting oxide that is well-known for its potential applications in catalysis, gas sensing, conducting electrodes, as well as in lithium batteries. The procedure for preparing PI/SnO_2 nanocomposite films is shown in Scheme 1, which includes (1) synthesis PAA solution with pyromellitic dianhydride (PMDA) and 4, 4′-oxidianiline (ODA); (2) subsequent ion exchange in ethanolic solution of stannous chloride ($SnCl_2$); (3) and final thermal treatment in air, during which PAA imidized to PI and Sn^{2+} ions oxidized into SnO_2 simultaneously, forming continuous tin oxide layers on PI surface. We show that surface morphology and thickness of the final metal oxide nanolayers on polymer surfaces can be controlled by ions loading contents and thermal treating processes. We expect that this direct ion-exchange and in situ oxidation processes could be extended to large scale fabrication of various metal oxides layers onto a flexible PI substrate aiming for a variety of potential applications.

EXPERIMENTAL SECTION

Materials. PMDA was purchased from Acros Organics and purified by sublimation treatment. ODA was obtained from Shanghai Research Institute of Synthetic Resins and recrystallized in ethyl acetate prior to use. *N*,*N*-Dimethylacetamide (DMAc) (analytical pure, ≤0.1% water) was purchased from Tianjin FuChen Chemicals Reagent Factory and used after distillation. Stannous chloride (analytic pure, ≥98% content) was produced from Tianjin YingDa Rare Chemical Reagents Factory and used as received. Alcohol (analytic pure, ≥99.5% content) was produced by Beijing Chemical Works and used as received.

Preparation of PI/SnO_2 Nanocomposite Films. The synthesis of PAA solution was performed by first dissolving the ODA in DMAc and then adding the PMDA with a 1% (mol/mol) offset of dianhydride gradually. After being stirred at room temperature for 2 h, a yellow viscous resin solution at 12 wt % solid content in DMAc was prepared. Then the homogeneous precursor solution was cast on glass substrates. After remaining in slowly flowing air for about 72 h to evaporate most of solvent, films with thicknesses of 50−60 μm were peeled from the glass substrates and immerged into ethanolic solution of $SnCl_2$ to conduct ion-exchange reactions. The tin(II)-containing PAA films were rinsed with alcohol and then thermally cured under tension in a forced-air oven. The curing circles can be found below. Initially, the tin(II)-containing PAA films were slowly heated up to 135 °C and held for 1 h at 135 °C to evaporate residual solvent. Then the films were heated up to higher temperature to oxidize tin(II) to SnO_2 and imidize PAA to PI.

$$\text{room temperature} \xrightarrow{1\text{h}} 135\ ^\circ\text{C for 1 h} \xrightarrow{2\text{h}} 350\ ^\circ\text{C for 5 h}$$

Characterization. The amount of Sn^{2+} loaded into PAA films was quantified by Seiko Instrument SPS 8000 inductively coupled plasma (ICP) atomic emission spectrometer. Samples were cut into squares (1.0 cm × 1.0 cm) and dissolved into concentrated nitric acid solution.

Attenuated total reflection-Fourier transform infrared (ATR-FTIR) spectra of the films between 4000 and 650 cm^{-1} were recorded on Nicolet Nexus 670 IR spectrometer with variable angle horizontal accessory, on which a 45° rectangle ZnSe crystal was used.

X-ray diffraction (XRD) of the nanocomposite films were performed using an X-ray diffractometer (D/Max2500VB2+/PC, Rigaku, Japan). The X-ray beam was generated by a Cu Kα target (λ = 1.5406 Å), using a tube voltage of 40 kV and a current of 200 mA. All samples had a scanning angle between 5° and 90°.

Thermal gravimetric analysis (TGA) was conducted on a Netzsch STA 449C system with a heating rate of 10 °C·min^{-1} in air. Mechanical properties were determined with an Instron-1185 system.

Scanning electron microscopy (SEM) images were obtained on an SEM-4700 Hitachi, Japan, at an accelerating voltage of 20 kV after samples were coated with ca. 5 nm of palladium−gold alloy. Transmission electron microscopy (TEM) was performed on an H-800 type Hitachi instrument at an operating voltage of 200 kV. The samples were prepared by adhering the film on a polyvinyl chloride board followed by cutting it perpendicular to the film surface using an ultramicrotome. These thin sections floating on a water bath were mounted onto the carbon-coated TEM copper grids for analysis. The adhesion between surface SnO_2 layers and polyimide substrate was evaluated by a scotch tape peeling test according to ASTM-3359B.

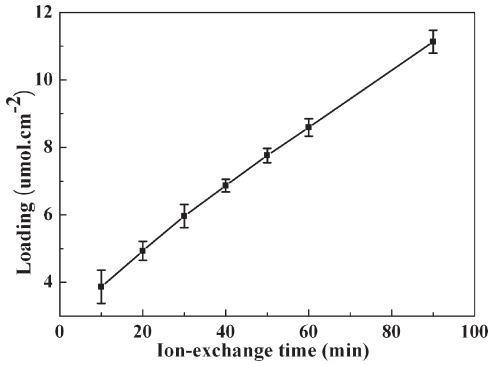

Figure 1. Amount of Sn^{2+} ions incorporated in PAA films via ion-exchange reactions in 0.1 M ethanolic solution of $SnCl_2$ as a function of ion exchange time.

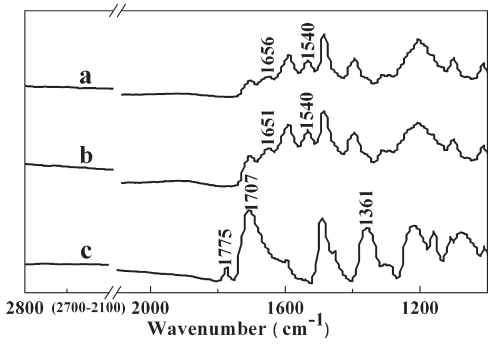

Figure 2. ATR-FTIR spectra of (a) PAA film, (b) Sn^{2+}−PAA film obtained by ion exchange in ethanolic solution of $SnCl_2$ for 60 min, and (c) final PI/SnO_2 composite film after thermal treatment of b at 350 °C for 1 h.

RESULTS AND DISCUSSION

Preparation of PI/SnO_2 Nanocomposite Films. Preparation of PI/SnO_2 nanocomposite films involves synthesis of PAA film containing carboxylic acid groups that can act as ion-exchangeable sites for the incorporation of Sn^{2+} into PAA films in a subsequent step and thermal treatment which led to formation of SnO_2 nanoparticles and imidization of PAA to PI simultaneously. The overall reaction processes are suggested as follows:

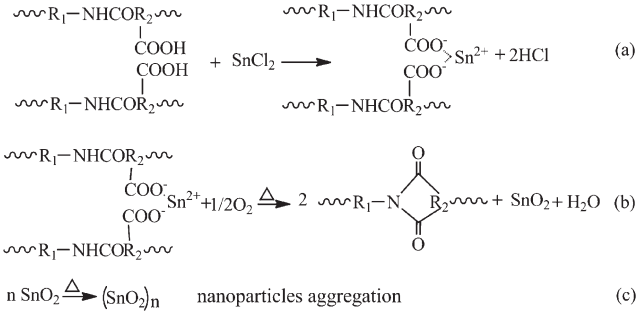

As shown in Scheme 1, Sn^{2+} was stoichiometrically incorporated into PAA substrate through ion-exchange reactions with hydrogen ions of carboxylic acid groups in a 1:2 molar ratio. The total amount of loaded Sn^{2+}, measured by ICP measurement, could be controlled simply by varying initial PAA film's immersion time in certain concentration of ethanolic solution of $SnCl_2$. As shown in Figure 1, the amount of Sn^{2+} ions in PAA film was

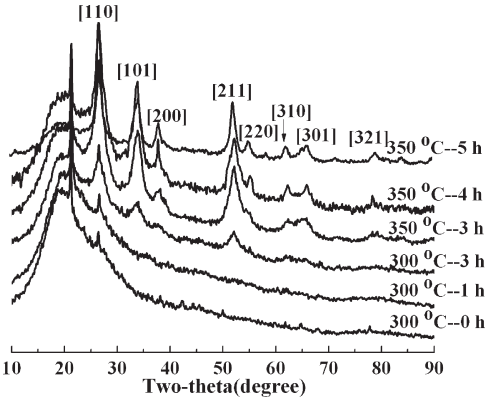

Figure 3. XRD patterns of PI/SnO_2 composite films obtained by ion-exchange in 0.1 M ethanolic solution of $SnCl_2$ for 60 min and followed by different thermal treatment processes.

linear increase with ion-exchange time. This linear dependence is caused by increasing the ion-exchangeable sites of PAA film linearly with increase immersion time. Sn^{2+} loading would play an important role in determining the morphology of metal oxide layers. We will discuss it in detail below.

Changes in chemical structure of polymeric films during whole procedures were similar to that of silvered PI films which we previously reported via the direct ion-exchange technique.[34] Figure 2 shows ATR-FTIR spectra of PMDA-ODA-based films during different treating processes. The bands at 1656 cm^{-1} (amide I; C═O stretching) and 1540 cm^{-1} (amide II; N—H mixed mode) amide observed from Figure 2a was characteristic bands of pristine PAA film. Little obvious difference is found between the spectrum of pristine PAA film and that of Sn^{2+}-doped film which is shown in Figure 2b. After thermal treatment at 350 °C for 1 h, the bands at 1775, 1707, and 1361 cm^{-1}, corresponding to symmetric C═O stretching, antisymmetric C═O stretching, and C—N—C stretching vibrations of imide structures, respectively, are the characteristic bands of PI due to imidization of PAA.

As shown in Figure 3, for thermal cured to 300 °C for 1 h, the XRD pattern shows only a very weak reflection (110) for SnO_2, and the film presents yellow appearance which is consistent with color of parent PI films. Further extending thermal treatment time to 3 h at 350 °C, one can clearly observe five reflections (110), (101), (200), (211), and (301) corresponding to the major characteristic peaks of tetragonal SnO_2 and the film presents black metallic luster which is consistent with inherent color of SnO_2 layers. For the film further thermal treated at 350 °C for 4 h, the five intense reflections became quite sharp and the new reflections (220), (310), and (321) of tetragonal SnO_2 became obvious too, which indicates generating of larger and more perfect tetragonal SnO_2 crystallites. It is very important to note that when the films further being heated to 350 °C for 5 h, though its XRD pattern is quite similar to that of 350 °C for 4 h, the films were found very brittle and lost their flexibility. This phenomenon is most probably caused by SnO_2 nanoparticles catalyzed oxidative degradation of PI matrix. The metal-oxide-catalyzed oxidative degradation of PI matrix was also reported in several studies on PI nanocomposites containing metal oxides such as ZnO and cobalt oxide nanoparticles.[35,36] No obvious diffraction peaks corresponding to other inorganic particles were detected throughout whole curing procedure, indicating that thermal treatment at 350 °C for 4 h is enough to form pure tetragonal SnO_2 particles in final PI composite films.

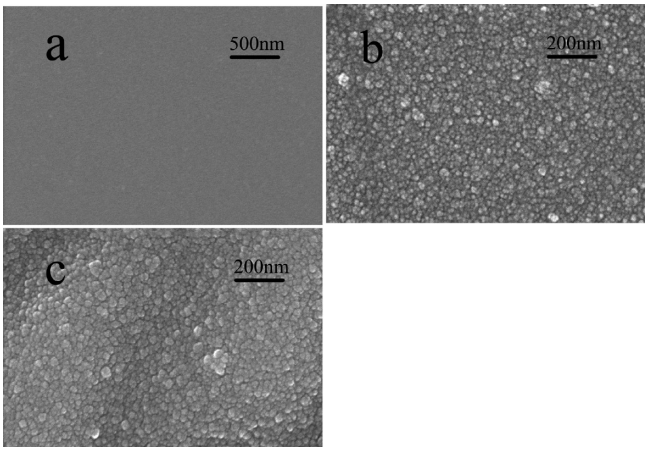

Figure 4. SEM images of parent PI film (a) and PI/SnO_2 composite films obtained by ion exchange in 0.1 M ethanolic solution of $SnCl_2$ for (b) 20 and (c) 60 min and followed by thermal treatment at 350 °C for 4 h in air.

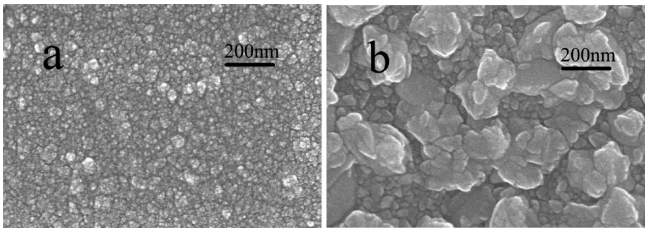

Figure 5. SEM images of PI/SnO_2 composite films obtained by ion exchange in (a) 0.2 and (b) 0.4 M ethanolic solution of $SnCl_2$ for 60 min and followed by thermal treatment at 350 °C for 4 h in air.

Surface Morphology of PI/SnO_2 Films and Adhesion Properties between the PI Matrix and SnO_2 Layers. As we mentioned above in Figure 1, ion-exchange time was an effective way to control Sn^{2+} loading contents in precursor films, which would determine structure and morphology of metal oxide layers of final composite films. Figure 4 shows SEM micrographs for samples conducted treatment time in ethanolic solution of $SnCl_2$ with various time, then followed by thermal treatment at 350 °C for 4 h in air. For the precursor films conducted ion exchange for 20 min, there were closely packed SnO_2 nanoparticles, only ca. 10−20 nm uniformly distributed on the film surface. After being ion exchange for 1 h, SnO_2 particles on the film surface have an average size of ca. 20−40 nm.

Morphology of final composite films can also be controlled by changing the concentrations of ethanolic solution of $SnCl_2$. Figure 5 shows SEM micrographs for samples were obtained by ion exchange in various concentrations of ethanolic solutions of $SnCl_2$, then thermal treatment at 350 °C for 1 h in air. It is clearly shown that SnO_2 particles altered with $SnCl_2$ concentrations. For the film ion-exchanged in 0.1 M solution for 1 h (Figure 5a), well-defined SnO_2 nanoparticles with an average size of 30 nm were formed. Further increased concentration to 0.4 M, one can clearly see that SnO_2 nanoparticles aggregated significantly and had an average size of ca. 100−200 nm (Figure 5b). However, these much bigger aggregated SnO_2 particles still consist of many smaller SnO_2 nanoparticles and the final film also showed a rough surface. Different morphologies of final nanocomposite films were caused by different content of Sn^{2+} loading. Higher concentration of ethanolic solution of $SnCl_2$ results in higher contents of Sn^{2+} loading in PAA films, which would lead SnO_2 agglomeration on PI substrate. Thus, 0.1 M ethanolic solution of $SnCl_2$ can meet the demand of our fabrication of PI/SnO_2 nanocomposite films.

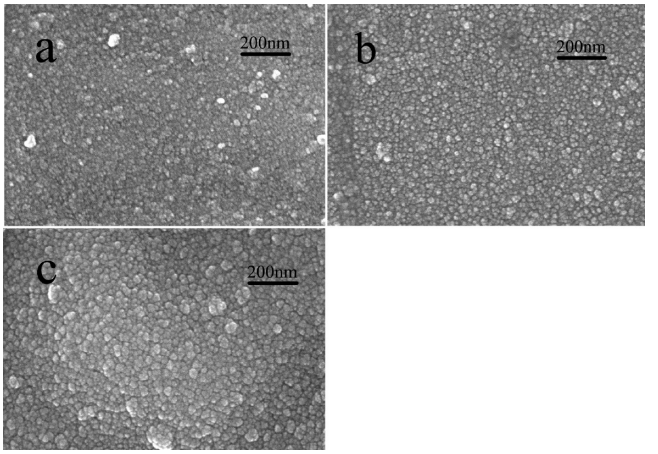

Figure 6. SEM images of PI/SnO_2 composite films obtained by ion exchange in 0.1 M ethanolic solution of $SnCl_2$ for 60 min and followed by thermal treatment at 350 °C for (a) 0, (b) 1, and (c) 4 h.

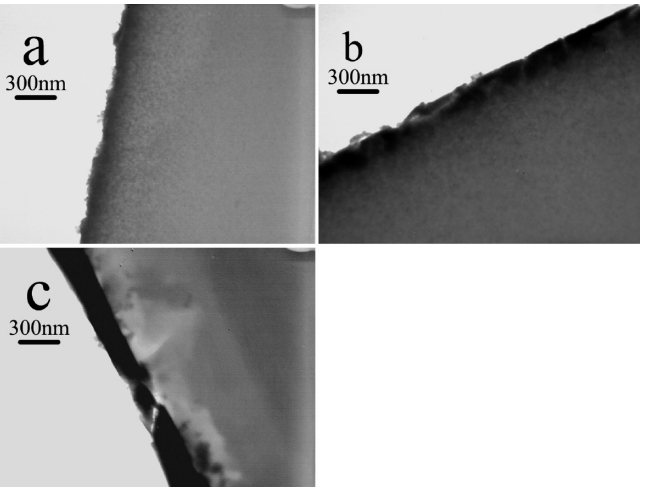

Figure 7. Cross-sectional TEM images of PI/SnO_2 composite films obtained by ion exchange in 0.1 M ethanolic solution of $SnCl_2$ for 60 min and followed by thermal treatment at 350 °C for (a) 0, (b) 1, and (c) 4 h.

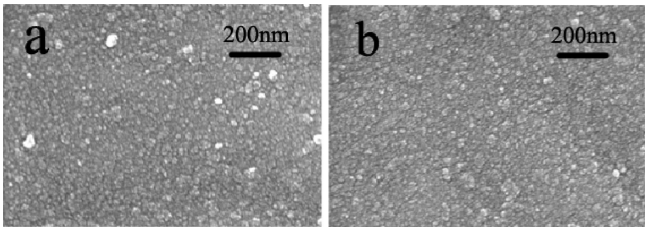

Figure 8. SEM images of PI/SnO_2 nanocomposite films (a) before and (b) after peeling off with adhesive tapes, The samples were obtained by ion exchange for 60 min in 0.1 M ethanolic solution of $SnCl_2$ and followed by thermal treatment at 350 °C for 1 h.

As shown in Figure 6, we can see that SnO_2 particles were altered with various thermal treating time. When we elevated

Table 1. Thermal and Mechanical Properties of Selected PI/SnO_2 Composite Films

samples[a]	tensile strength (MPa)	elongation (%)	modulus (MPa)	10%-WLT in Ar (°C)[b]	10%-WLT in air (°C)[c]
parent PI	77.9	22.83	952.7	591	578
ion-exchange for 30 min	79.1	15.32	956.8	567	566
ion-exchange for 60 min	85.8	14.61	984.7	553	553

[a] All samples were thermally treated at 350 °C for 4 h. [b] 10%-weight-loss temperature in Ar. [c] 10%-weight-loss temperature in air.

thermal treatment temperature to 350 °C, Figure 6a shows the distribution of SnO_2 particles with an average size of ca. 10−15 nm. As extending treatment time to 1 h, SnO_2 nanoparticles have an average size of ca. 20−30 nm, which suggests SnO_2 nanoparticles aggregation on surfaces of PI films. We suggested that SnO_2 nanoparticles diffused to surfaces of PI films and agglomerated there. The diffusion of newly SnO_2 nanoparticles could be clearly observed through TEM measurement. Figure 7a and b show that SnO_2 layers are formed on surfaces of PI films and that a lot of SnO_2 nanoparticles remained in the bulk polymer matrix. When thermal treatment at 350 °C for 4 h, Figure 7c shows that the surface layer of SnO_2 is continuous with ca. 150−280 nm thick and only a few SnO_2 nanoparticles distributed in the bulk polymer matrix.

Figure 8 shows SEM images of surface SnO_2 modified PI nanocomposite films before and after a peeling test as a qualitative evaluation of bonding strength between SnO_2 particles and PI matrix.[32] After the peeling test (Figure 8b), compared with before peeling (Figure 8a), the peeling became negligible and no obvious peeling spots were observed. Adhesion of metal oxide to polyimide is acceptable. Electron microscopy data suggests that the strong adhesion is due to a mechanical interlocking mechanism.[37]

Thermal and Mechanical Properties. Thermal and mechanical property characterizations were carried out on PI/SnO_2 composite films. As displayed in Table 1, no matter in air or in Ar atmosphere, 10% weight-loss temperatures of composite films are similar to that of pristine PI. The mechanical properties in Table 1 show that SnO_2 nanoparticles embedded in PI matrix do not diminish the bulk PI framework significantly. Though the elongation at break of nanocomposite films is a little lower than that of pristine PI, tensile strength, and modulus increased because a few of SnO_2 nanoparticles are embedded in PI matrix, which leads to nanoparticles reinforced composite materials. Both thermal and mechanical data suggest that composite films retain essential properties of pristine PI, which would probably attribute to the intact inner bulk of the PI matrix.

CONCLUSION

SnO_2 nanolayer-modified PI composite films were successfully prepared by direct ion-exchange and in situ oxidation process. The nanocomposite films are prepared by loading Sn^{2+} into pure PAA films, through ion exchange reactions of damp-dry PAA films in ethanolic solution of $SnCl_2$. Subsequent thermal treatment in air results in imidization of PAA to PI and simultaneous oxidation of Sn^{2+} to SnO_2, forming continuous SnO_2 layers on PI films. Ion loadings provide control over the microstructure of the PI/SnO_2 nanocomposite films. The adhesion between surface SnO_2 layers and polyimide matrix is acceptable. The nanocomposite films basically maintained the thermal and mechanical properties of the pristine PI matrix. This work may demonstrate that this direct ion-exchange and in situ oxidation process is a powerful methodology for fabricating PI nanocomposite films combined with a variety of functional metal oxides.

AUTHOR INFORMATION

Corresponding Author

*E-mail: wuzp@mail.buct.edu.cn. Tel.: +86-10-64421693. Fax: +86-10-64421693.

ACKNOWLEDGMENT

This research was financially supported by the National Natural Science Foundation of China (NSFC, Project 50973006) and the Program for Changjiang Scholars and Innovative Research Team in University (PCSIRT, IRT0706).

REFERENCES

(1) Guillén, C.; Herrero, J. *Phys. Stat. Solidi (a)* **2010**, *207*, 1563–1567.
(2) Shirahata, N.; Hozumi, A. *Chem. Mater.* **2005**, *17*, 20–27.
(3) Leonardo, G. P.; Fernando, J. F.; Alcantara, G. B.; Maria, A. G. S.; Morais, P. C.; Sinnecker, J. P.; Novak, M. A.; Lima, E. C. D.; Leite, F. L.; Mattoso, C. *Thin Solid Films* **2009**, *517*, 1747–1752.
(4) Joseph, T. D.; Schwartz, J. *ACS Appl. Mater. Inter.* **2009**, *1*, 2119–2122.
(5) Simeone, D.; Minotti, A.; Mariucci, L.; Fortunato, G.; Pecora, A.; Maiolo, L.; Cuscuna, M. *Solid-State Electron.* **2008**, *52*, 348–352.
(6) Muylaert, I.; Borgers, M.; Bruneel, E.; Schaubroeck, J. *Chem. Commun.* **2008**, 4475–4477.
(7) Laskarakis, A.; Logothetidis, S.; Kassavetis, S.; Papaioannou, E. *Thin Solid Films* **2008**, *516*, 1443–1448.
(8) Kabra, D.; Myoung, H. S.; Wenger, B.; Friend, R. H.; Snaith, H. J. *Adv. Mater.* **2008**, 3447–3452.
(9) Kima, H. S.; Sohna, B. H.; Leeb, W.; Leeb, J. K.; Choia, S. J.; Kwon, S. J. *Thin Solid Films* **2002**, *419*, 173–177.
(10) Drew, C.; Liu, X.; Ziegler, D.; Wang, X. Y.; Ferdinando, F. B.; Whitten, J.; Samuelson, L. A.; Kumar, J. *Nano Lett.* **2003**, *3*, 143–147.
(11) Cooper, R.; Hari, P. U.; Minton, T. K.; Berman, M. R.; Du, X. H.; Steven, M. G. *Thin Solid Films* **2008**, *516*, 4036–4039.
(12) Prandi, J.; Namy, J. L.; Huang, H.; Linda, F. N. *Angew. Chem., Int. Ed.* **2001**, 3880–3884.
(13) Li, T. L.; Hsu, S. L. C. *Eur. Polym. J.* **2007**, *43*, 3368–3373.
(14) Calnan, S.; Upadhyaya, H. M.; Thwaites, M. J.; Tiwari, A. N. *Thin Solid Films* **2007**, *515*, 6045–6050.
(15) Peiro, A. M.; Ravirajan, P.; Govender, K.; David, S. B.; Paul, O. B.; Donal, C. B.; James, R. D. *J. Mater. Chem.* **2006**, *16*, 2088–2096.
(16) Taek, A.; Choi, Y. J.; Yi, M. H. *Appl. Surf. Sci.* **2008**, *255*, 2185–2191.
(17) John, A. K.; James, R. E. *Adv. Mater.* **1998**, *10*, 1229–1232.
(18) Hasegawa, M.; Horie, K. *Prog. Polym. Sci.* **2001**, *26*, 259–355.
(19) Zhan, J. Y.; Tian, G. F.; Jiang, L. Z.; Wu, Z. P.; Wu, D. Z.; Yang, X. P.; Jin, R. G. *Thin Solid Films* **2008**, *516*, 6315–6320.
(20) Rameev, B.; Okay, C.; Yildiz, F.; Khaibullin, R. I.; Popok, V. N.; Aktas, B. *J. Magn. Magn. Mater.* **2004**, *278*, 164–171.
(21) Stergios, L. *Mat. Sci. Eng. B-Solid* **2008**, *152*, 96–104.
(22) Johann, B.; Jenny, N. *J. Mater. Chem.* **2007**, *17*, 3141–3153.
(23) Craig, M. T.; Helen, M. H.; Thomas, S. G.; John, W. C. *Compos. Sci. Technol.* **2003**, *63*, 1591–1598.

(24) Bergmeister, J. J.; Rancourt, J. D.; Taylor, L. T. *Chem. Mater.* **1990**, *2*, 640–641.
(25) Bergmeister, J. J.; Rancourt, J. D.; Taylor, L. T. *Chem. Mater.* **1992**, *4*, 729–737.
(26) Tsai, M. H.; Huang, S. L.; Chen, P. J.; Chiang, P. C.; Chen, D. S.; Lu, H. H.; Chiu, W. M.; Chen, J. C.; Lu, H. T. *Desalination* **2008**, *233*, 232–238.
(27) Somwangthanaroj, A.; Suwanchatchai, K.; Ando, S.; Tanthapanichakoon, W. *Mater. Chem. Phys.* **2009**, *114*, 751–755.
(28) Qiu, W. L.; Luo, Y. J.; Chen, F. T.; Duo, Y. Q.; Tan, H.M.. *Polymer* **2003**, *44*, 5821–5826.
(29) Chiang, P. C.; Whang, W. T.; Tsai, M. H.; Wu, S. C. *Macromolecules* **2004**, *448*, 359–364.
(30) Chiang, P. C.; Whang, W. T. *Polymer* **2003**, *44*, 2249–2254.
(31) Mu, S. X.; Wu, D. Z.; Wang, Y.; Wu, Z. P.; Yang, X. P.; Yang, W. T. *ACS Appl. Mater. Inter.* **2010**, *2* (1), 111–118.
(32) Wu, Z. P.; Wu, D. Z.; Yang, W. T.; Jin, R. G. *J. Mater. Chem.* **2006**, *16*, 310–316.
(33) Yang, S. Q.; Wu, D. Z.; Qi, S. L.; Cui, G. H.; Jin, R. G.; Wu, Z. P. *J. Phys. Chem. B* **2009**, *113*, 9694–9701.
(34) Qi, S. L.; Wu, Z. P.; Wu, D. Z.; Wang, W. C.; Jin, R. G. *Chem. Mater.* **2007**, *19*, 393–401.
(35) Hsu, S. C.; Whang., W. T.; Hung, C. H.; Chiang, P. C.; Hsiao, Y. N. *Macromol. Chem. Phys.* **2005**, *206*, 291–298.
(36) Mu, S. X.; Wu, Z. P.; Wang, Y.; Qi, S. L.; Yang, X. P.; Wu, D. Z. *Thin Solid Films* **2010**, *518*, 4175–4182.
(37) Robin, E. S.; David, W. T. *Adv. Mater.* **1999**, *11*, 1043–1047.